aurum

AURUM MÜHENDİSLİK SİSTEMLERİ VE MİMARLIK DERGİSİ
AURUM JOURNAL OF ENGINEERING SYSTEMS AND ARCHITECTURE

Cilt 5, Sayı 2 | Kış 2021
Volume 5, No 2 | Winter 2021, 237-259

ARAŞTIRMA MAKALESİ / RESEARCH ARTICLE

THERMAL PERFORMANCE IMPROVEMENT OF SHELL AND HELICAL COIL HEAT EXCHANGER

Tareq H. ABED[1]
[1]Mechanical Engineering Department, Institute of Graduate Studies, Altınbaş University, İstanbul-Turkey
tareq.abed@ogr.altinbas.edu.tr, ORCID No: 0000-0003-4610-3139

İbrahim KOÇ[2]
[2]Mechanical Engineering Department, Institute of Graduate Studies, Altınbaş University, İstanbul-Turkey
ibrahim.koc@altinbas.edu.tr, ORCID No: 0000-0002-1379-7093

GELİŞ TARİHİ/RECEIVED DATE: 12.09.2021 KABUL TARİHİ/ACCEPTED DATE: 01.12.2021

Abstract

Nowadays, energy consumption increases so it is necessary to enhance the efficiency and performance of heat energy transition. The effects of perforated twisted tape on heat transfer coefficient, effectiveness, Nusselt number, and pressure drop are studied numerically. Modeling of heat exchanger with the perforated twisted tape is applied where finite volume method is utilized to perform the setup and complete the solution. The numerical results are validated with previous experimental results and there is an excessive agreement between the numerical and experimental results. The range of Reynolds numbers is from 3800 to 18000. The results showed that the overall heat transfer coefficient U increases with the rise of Reynolds number where the perforated twisted tape achieves the maximum enhancement of heat transfer coefficient achieving the numbers from 965 to 1250 W/m^{2}K. The perforated twisted tape has the highest ratio of enhancing Nusselt number following the numbers from 65 to 115 and this can be explained as the velocity rises, the turbulence level increases. Heat exchanger effectiveness increases with the growth of Reynolds number where the perforated twisted tape attained the supreme enhancement of effectiveness reaching the numbers from 0.35 to 0.85. It is indicated that the twisted tape configuration has the maximum ratio of pressure drop increase as the complicity of twisted tape rise the pressure drop. Contours and streamlines of hot and cold water cross the heat exchanger explains the distributions of temperature, velocity, and pressure.

Keywords: Heat exchanger, Perforated twisted tape, Thermal performance

KABUK VE SARMAL BOBİN ISI EŞANJÖRÜNÜN TERMAL PERFORMANSININ İYİLEŞTİRİLMESİ

Özet

Günümüzde enerji tüketimi arttığı için ısı enerjisi geçişinin verimliliğini ve performansını artırmak gerekmektedir. Delikli bükümlü bandın ısı transfer katsayısı, etkinlik, Nusselt sayısı ve basınç düşüşü üzerindeki etkileri sayısal olarak incelenmiştir. Kurulumu gerçekleştirmek ve çözümü tamamlamak için sonlu hacim yönteminin kullanıldığı ısı eşanjörünün delikli bükümlü bant ile modellenmesi uygulanmıştır. Sayısal sonuçlar önceki deneysel sonuçlarla doğrulanmıştır ve sayısal ve deneysel sonuçlar arasında aşırı bir uyum vardır. Reynolds sayılarının aralığı 3800 ila 18000 arasındadır. Sonuçlar, genel ısı aktarım katsayısının U'nun, Reynolds sayısının artmasıyla arttığını göstermiştir; burada delikli bükümlü bant, 965 ila 1250 W/ sayılarına ulaşarak ısı aktarım katsayısında maksimum artış sağlar. m2K. Delikli bükümlü bant, 65'ten 115'e kadar olan sayıların ardından Nusselt sayısını arttırma oranı en yüksek olanıdır ve bu, hız arttıkça türbülans seviyesi arttıkça açıklanabilir. Isı eşanjörünün etkinliği, delikli bükümlü bandın 0.35'ten 0.85'e ulaşan sayılara ulaşan üstün etkinlik geliştirmesine ulaştığı Reynolds sayısının büyümesiyle artar. Bükümlü bandın karmaşıklığı basınç düşüşünü artırdıkça, bükümlü bant konfigürasyonunun maksimum basınç düşüşü artış oranına sahip olduğu belirtilmektedir. Isı eşanjöründen geçen sıcak ve soğuk suyun hatları ve akış çizgileri sıcaklık, hız ve basınç dağılımlarını açıklar.

Anahtar Kelimeler: Eşanjör, Delikli bükümlü bant, Termal performans

1. INTRODUCTION

Heat exchangers are essential components in a variety of industrial processes, including heat ventilation and air conditioning, petroleum processing, refrigeration, and food preparation. Shell and helically coiled tube heat exchangers, which are typically made up of helically coiled tubes and a cylindrical shell, are some of the most extensively used heat exchangers in the applications stated. Many investigations have been conducted on the heat transfer process in various sorts of heat exchangers. In comparison to straight tube heat exchangers, shell and helically coiled heat exchangers were beneficial as heat transfer equipment due to their compact and higher heat transfer coefficients.(Chagny et al., 2000). improved the performance of a shell and helically coiled heat exchanger by incorporating a hollow tube into the shell side, which allows cold fluid to enter the heat exchanger. Numerical simulation was used to evaluate the performance of a modified shell and helically coiled heat exchanger to that of a typical vertical shell and helically coiled heat exchanger. The result of the study demonstrated that the redesigned heat exchanger was successfully designed. In general, incorporating a hollow tube into the heat exchanger's shell side resulted in increased heat transfer by regulating fluid flow in the shell side. In the run, the overall heat transfer coefficient was determined. The overall heat transfer coefficient was found to be between 1600 and 3150 W/m2K. In addition, the heat transfer coefficient of the coil side was found to be in the range of 5700–13400 W/m2K in this investigation. Furthermore, there was an average variation of 8% between simulation and experimental data.(Manglik & Bergles, 2003) finished an analysis of the use of twisted-tape inserts in tubular heat exchangers and their thermal-hydraulic performance. Twisted tapes improve heat transmission by creating swirl or secondary flows, increasing flow velocity owing to tube partitioning and obstruction, and essentially extending the helical flow length. Fin effects may be present depending on the tape-edge to tube-wall contact. The use of these

materials in single-phase and two-phase (boiling and condensation) flows is discussed, and heat transfer and pressure drop findings from several studies were shown. The nature of swirl flows and their scaling, as well as the establishment of predicted correlations for heat transfer coefficients and friction factors (or pressure drop), were all examined. Also briefly described were certain features of the usage of geometrically modified twisted-tape inserts, as well as compound application with other enhancing techniques. Using computational fluid dynamics(Galeazzo et al., 2006). investigated a virtual prototype of a four-channel plate heat exchanger with flat plates (CFD). Experimental findings were compared to numerical estimates for heat load produced from a 3D CFD model as well as a 1D plug-flow model using parallel and series flow configurations. The CFD model represents the exchanger's channels, plates, and conduits, as well as the uneven flow distribution between channels and flow maldistribution inside the channel. The CFD results, particularly for the series arrangement, were in good accord with experimental data. In a concentric double tube heat exchanger (Eiamsa-Ard & Promvonge, 2007). evaluated the effects of inserting a helical screw-tape with or without a core-rod on heat transfer and flow friction characteristics. The loose-fit helical tape, with or without core-rod, was put in the inner tube of the heat exchanger in the experiment, and hot water was pumped into the tube based on its Reynolds number, which ranges from 2000 to 12,000. The loose-fit, helical tape with and without core-rod raises the average Nusselt number by 230 % and 340 %, respectively, over the comparable plain tube, according to the testing data. It's worth noting that the friction factor for the loose-fit, helical tape without core-rod was around half that of the one with core-rod, while the Nusselt number was around half that of the one with core-rod. Furthermore, for tapes with and without core-rod, the enhancement efficiency of helical screw-tapes varies between 1.00 and 1.17, 1.98 and 2.14, respectively (Salimpour, 2009), conducted experimental research on the heat transfer coefficients of shell and helically coiled tube heat exchangers. For both parallel-flow and counter-flow arrangements, three heat exchangers with varied coil pitches were chosen as test sections. Using suitable equipment, all needed parameters such as intake and outlet temperatures of tube-side and shell-side fluids, a flow rate of fluids, and so on were measured. The predicted tube-side heat transfer coefficients were also compared to existing heat transfer coefficients for different boundary circumstances, and a satisfactory agreement was found. (Moawed, 2011), experimented with forced convection from the outside surfaces of helical coiled tubes with a constant wall heat flow. The studies were carried out in a suction-mode open-circuit airflow wind tunnel device. The results of the experiments revealed that these variables have a significant impact on the average heat transfer coefficient. At constant Re and P/do, the average Nusselt number (Num) grows as D/do grows. At constant Re and D/do, Num also grows when P/do grows. There was a lot of consistency between the current experimental results and earlier studies. Re, D/do, and P/do were all connected to the average Nusselt values (Panahi & Zamzamian, 2017), investigated the effect of a helical wire put within a helically coiled tube as a turbulator experimentally. Experiments were conducted in two different ways. The fluid of the coiled tube was water in the first mode and air in the second mode. Each scenario was investigated for an empty coiled tube (without turbulator) and a coiled tube with turbulator at various fluid flow rates. For all cases, the fluid on the shell side was hot water. The results revealed that this form of turbulator may be used in coiled tubes, resulting in a considerable increase in the total heat transfer coefficient and, therefore, pressure decrease.

Heat transfer coefficient, pressure drop, efficacy, and the number of transfer units (NTU) were all analyzed and addressed. In steady-state forced convection heat transfer in shell and helically coiled tube heat exchangers (Alimoradi & Veysi, 2017), computed the heat transfer and entropy production. The effect of geometrical heat exchanger parameters such as tube diameter, coil diameter, the diameter of the inlet of shell, shell diameter, the height of the coil, height of the shell, pitch, and distance between the inlet and outlet of the shell on heat transfer rate and entropy generation has been investigated simultaneously. These parameters have been determined to have critical and ideal values that reduce and maximize the heat transfer rate per entropy generation. (Agbossou et al., 2018), focused on the true shape of the heat exchanger and the energy retrieved from the ground in a 3D finite element model of helical coil Ground Heat Exchangers (GHE). The created model was applied to a single GHE as well as numerous GHEs. The results suggest that operating the GHE in an intermittent short time mode increases its performance. In the case of several GHEs, the best spacing between them (of 1 m diameter) was at least 4 times the GHEs diameter for line or square configurations and 6 times the GHEs diameter for hexagonal configurations, according to the research. Outside of the basic assumptions of the standard 2D axisymmetric models, the created 3D Finite Element model might be useful in exploring helical coil GHE difficulties. (Sepehr et al., 2018), used numerical simulations to investigate heat transmission, pressure drop, and entropy creation in shell and helically coiled tube heat exchangers. The heat transmission rate was increased by placing annular fins on the coiled tube's outer surface. The height and number of fins, as well as the velocity of the fluid on the shell side, fluctuate. The study's primary findings include some recommended correlations for estimating the Nusselt number and friction factor of the shell side. The link between the NTU, the rate of entropy formation, and the thermal efficacy were also determined. The model was confirmed by comparing the numerical values of both sides' Nusselt numbers, as well as the friction factor on the coil side, to the expected values based on past empirical correlations. A sample issue was established and answered in the concluding portion of this research as a guide for the designer of these sorts of heat exchangers. (Sharifi et al., 2018), investigated the effect of wire coil inserts inside heat exchangers at various Reynolds numbers. A significant effort was undertaken to construct structural hexahedral meshes across all of the heat-exchanger geometries to get trustworthy and confirmed findings. The verified models then clarified the object and circumstances that would optimally enhance heat transmission in twin pipe heat exchangers. The results of this study show that using suitable wire coils to enhance Nusselt values by 1.77 times was possible. Proper friction coefficient and Nusselt number correlations for various coiled wire inserts with varying geometric configurations under laminar flow were proposed as a result of the numerical simulation. The correlations in this study, unlike the previous ones, were based on the occupied spaces that helical wires occupy within tubes; hence, the two updated correlations may both be employed for nonuniform helical wire insert designs. (Niwalkar et al., 2019), improved the heat transfer coefficient in a shell and helically coiled tube heat exchanger using various volume concentrations of SiO2/water nanofluid, researchers. Hot nanofluid flows through the helical tube, while cold water flows through the shell side of the heat exchanger. The hot nanofluid's fluid flow rate was changeable. At 50 liters per hour, the cold water flow rate remains constant (LPH). The results reveal that raising the mass flow rate and %age volume concentrations of SiO2/water nanofluid boosted the heat transfer coefficients of nanofluids. When compared to water, the heat transfer

coefficient of SiO2/water nanofluids was 28.71 % greater. The heat transfer coefficient of SiO2/water nanofluid for a fluid flow rate of 50 LPH was 65.81 % and 82.46 % greater than for fluid flow rates of 30 and 40 LPH, respectively. When compared to water, the friction factor and pressure drop for SiO2/water nanofluids were 52.61 % and 62.60 % greater, respectively. (Palanisamy & Kumar, 2019), evaluated the heat transfer and pressure drop of a cone helically coiled tube heat exchanger Using multi-wall carbon nanotube (MWCNT)/water nanofluids. For the nanofluids volume concentrations of 0.1 %, 0.3 %, and 0.5 %, respectively, the experimental Nusselt number was 28 %, 52 %, and 68 % greater than water. The pressure decrease of 0.1 %, 0.3 %, and 0.5 % nanofluids was found to be 16 %, 30 %, and 42 % greater than that of water, respectively. It was discovered that handling MWCNT poses no immediate danger and that even after multiple test runs, there was no appreciable degradation of the coiled tube inner wall surface. As a result, MWCNT/water nanofluids were being used as a replacement for standard heat transfer fluids in cone helically coiled tube heat exchangers to enhance heat transmission while reducing pressure loss. (Abu-Hamdeh et al., 2020), investigated the thermal and hydraulic properties of sector-by-sector heat exchangers, a novel form of the helically coiled tube heat exchanger. The flow regime under investigation was turbulent. The effects of the Nusselt number and friction factor on the Reynolds number, sector angle and its orientation, dimensionless pitch, and coil diameter were investigated. Equations for estimating the Nusselt number and friction factor as functions of the specified parameters were proposed for each kind of heat exchanger. It was discovered that sector by sector heat exchangers with a semi-circular cross section were more efficient than quadrant-circular cross section and tube-in-tube heat exchangers. (G. Wang et al., 2020), employed helically coiled-twisted trilobal tube (HCTTT) in the heat exchanger. To comprehensively evaluate comprehensive performance, two evaluation criteria, performance evaluation criteria (PEC) and filed synergy number (Fc), were introduced. The results showed that the HCTTT performs better in the hydrodynamic and thermal performance than the helically coiled elliptical tube, helically coiled plain tube (HCPT), and trilobal tube (HCTT). According to the HCPT, the augmentation ratio of flow resistance was up to 24 % –38 %, while the Nusselt number of HCTTT was increased by more than 19 % –31 %. (Abu-Hamdeh et al., 2021) He looked into the exergy of fluid flow and thermal energy transfer inside the sector-by-sector and tube-in-tube (TIT) kinds of helically coiled heat exchangers (HCTHs). New formulae for estimating exergy efficiency and coefficient of exergy performance as functions of both sides have been proposed. Dimensionless coil diameter and pitch, Reynolds numbers. These equations were used to compwere the performance of these heat exchangers. Exergy efficiency decreases by 21.8 %, 25.7 %, and 21.1 %, and the coefficient of exergy performance decreases by 8%, 9.3%, and 14.8 % for heat exchangers with semi-circle cross section, quadrant-circle cross section, and TIT heat exchangers, respectively, when the dimensionless coil diameter was doubled. Furthermore, instead of the conventional TIT kinds, SBS heat exchangers with semi-circle and quadrant-circle cross sections were strongly suggested. (Farnam et al., 2021), improved the thermal efficiency of a coil heat exchanger using a helical tube by twisting the construction. The twisted walls prevent the formation of thermal boundary layers in the flow direction and modify the position and strength of created secondary flows and velocity contours constantly, resulting in a more uniform temperature. For a model with median levels of design characteristics, a 14.2% increase in Nusselt number and a 7.7% increase in friction factor were measured. The helical-diameter has the

greatest influence on the thermal–hydraulic parameters of the helical-twisted tube, whereas the twist-pitch and helical-pitch are second and third, respectively. As the helical diameter and twist pitch are reduced, the overall hydrothermal performance increases. At a Reynolds number of 900, the model with a helical diameter of 50 mm achieves the highest performance index of 1.98. (Rasheed et al., 2021), experimented and calculated three types of helical microtube coils: circular, oval, and elliptical. Working fluids and base fluids were Al2O3-water and ZnO-water at three volume fractions of 1.0 %, 1.5 %, and 2 %. For all geometries, several values of pitch were evaluated with a constant pitch/diameter ratio of 1. The results suggest that helical microtube curvature swirls were a key factor in increasing heat transmission. It also indicates that when the volume fractions of nanofluids and the Reynolds number grow, heat transmission and friction loss rise. The research also revealed that using helical microtubes significantly improves the heat transfer ratio, with the maximum improvement ratio achieved when using circular shape with = 2% alumina nanofluid. Alumina nanofluid outperformed ZnO-water nanofluid throughout a wide range of flow conditions, with the greatest thermal performance of 3.1 achieved at a Reynolds number of 1800 and alumina nanofluid at = 2%. In addition, based on experimental data, additional empirical correlations were hypothesized and published.

From the previous literature review, it is observed that many researchers studied the effects of different baffles configurations and nanofluids materials on helically tubed heat exchangers but fewer studies investigated inserts inside coils. Spring wire insert inside the tube was utilized but the perforated twisted tape of the helical tube's heat exchanger was not used. Many experimental studies were completed to investigate the performance of shell and helically tube heat exchangers but fewer numerical studies were indicated. In this study, the Finite element method is used to study the effects of twisted tape on heat exchanger performance such as Effectiveness, heat transfer coefficient, and pressure drop were studied numerically. Contours and streamlines of temperature, velocity, and pressure are extracted to have a deep understanding of the fluid motion and heat transfer distribution.

2. NUMERICAL STUDY

In this section, the three-dimensional model that is accomplished by cad software and perforated twisted tape of the helical tubes heat exchanger dimensions were introduced.

2.1 Helical Coil Heat Exchanger Modeling

The physical model that is utilized to simulate the motion of water inside the helical coil heat exchanger with a perforated twisted tape inserted inside the coil is illustrated in Fig.1.

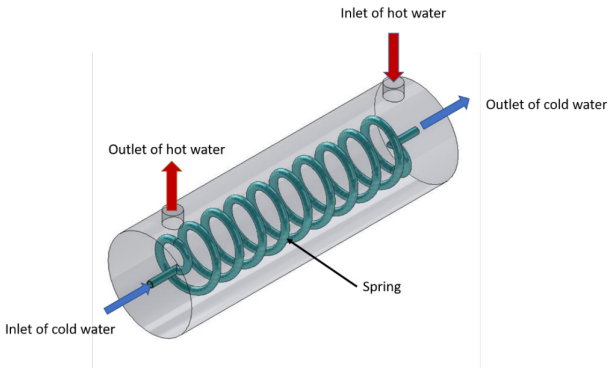

Figure 1. Three dimensions model of cold and hot sides.

The inlets and outlets of cold and hot water were illustrated in the figure where the cold water flows inside the helical coil and the hot water moves inside the shell side. The specifications of the helical coil that is fabricated from the copper material because of high thermal conductivity were investigated in Fig.2. The dimensions of the helical coil with 30 mm pitch is shown in Table 1.

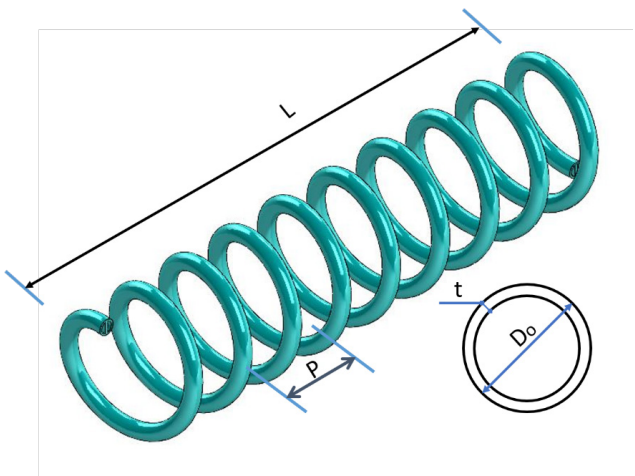

Figure 2. Three model of helical coil.

Table 1. Specifications and dimensions of helical coil

Parameters of helical coil	Dimensions
Spring length, L	285 mm
Spring pitch, P	30 mm
Number of revolutions, N	9.5
Outer tube diameter, D_o	8 mm
Tube thickness, t	1 mm

For heat transfer enhancement, perforated twisted tape has a rectangular cross-section inserted inside the helical coil as seen in Fig.3. More illustration for the tape and hole inside the tube is investigated in Fig.4 to show the contacts between them. Small holes with 2 mm diameter were distributed on the surface of the twisted tape. More specifications of perforated twisted tape were illustrated in Table 2.

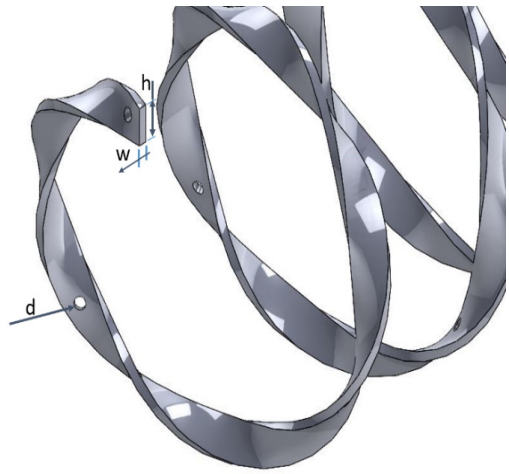

(a)

Figure 3. The specifications of perforated twisted tape.

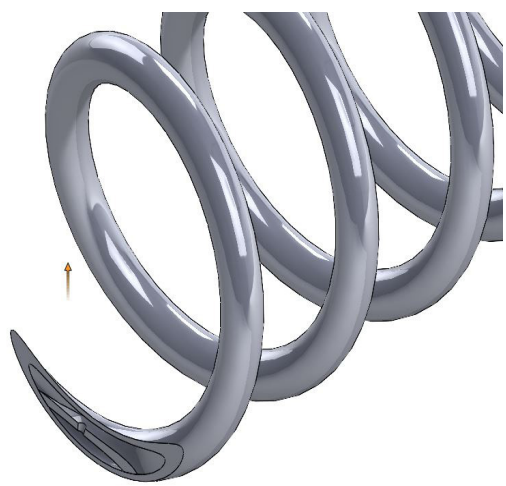

Figure 4. Shape of tape inside the coil.

Table 2. Specifications and dimensions of perforated twisted tape

Parameters of perforated twisted tape	Dimensions
Tape height, h	6 mm
Tape width, w	1.2 mm
Hole diameter, d	2 mm
Number of holes	30
Twisting angle	25°
Twisted tape pitch	30 mm

To study the effects of utilizing perforated tapes, three cases (only helical coil, twisted tape, perforated twisted tape) were performed as seen in Fig.5.

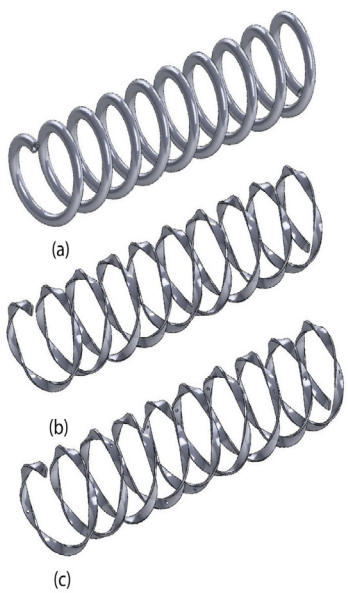

Figure 5. Test runs cases (a) only helical coil, (b) twisted tape, (c) perforated twisted tape.

2.2 Mesh Generation

A complicated system containing physical domains of a helical coil, perforated twisted tape, hot oil, and cold water has been meshed with an unstructured tetrahedron mesh in this work. Aside from the helical coil and perforated twisted tape, mesh enhancements were used. The mesh generation for the heat exchanger and the helical coil is shown in Fig. 6. To fulfill the mesh dependency check, three grid systems with 1.324, 1.854, and 2.561 million elements were created. Between the finest grid and the median number of grids, the inaccuracy in results values is less than 1.52 % and 2.27 %, respectively. As a result, the 2.561 million cell model was employed for these experiments. Table 3 shows the error %age of heat transfer coefficient and effectiveness for the three cases of grid generations.

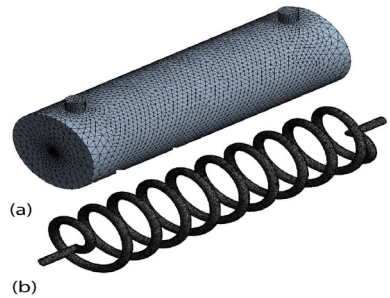

Figure 6. Mesh generation for (a) helical coil heat exchanger (b) helical coil.

Table 3. Error %age of heat transfer coefficient and effectiveness

Meshing elements number	U	Effectiveness	U Error %	Effectiveness Error %
1.324 million	995	0.472	2.023%	1.964%
1.854 million	997	0.479	1.351%	1.032%
2.561 million	998	0.481	0.098 %	0.087 %

2.3 Boundary and Initial Condition

For steady-state analysis, a commercial software tool (Jean et al., 2014) is utilized to build up and solve the mass and energy equations. For the viscous enhanced wall function model, a pressure-based solver was adopted with the gravity effect and a realizable k-ε. The number of simulation iterations required to produce a converged solution is determined by the mass continuity, velocity flow, energy, and turbulent viscosity solution. For pressure-velocity coupling, a simple approach is selected. The convective terms such as momentum, energy, and turbulent kinetic energy equations are discretized using the second-order unwinding methodology. For boundary conditions, a cold-water velocity input is assumed at the receiver's intake with the needed values, with the temperature set at 27 C° as seen in Table 4. The hot water inlet is considered to be at 50 C°. The outer surface of the heat exchanger is performed at zero heat flux to reach full insulation.

Table 4. Numerical boundary conditions

Boundary conditions	
Reynolds number range	3800 to 18000
Pressure outlet of hot water	Atmospheric pressure (101325 Pa)
Pressure outlet of cold water	Atmospheric pressure (101325 Pa)
Heat flux of outer surfaces	0.0
Inlet cold water temperature	27 C°
Inlet hot water temperature	50 C°

3. DIMENSION REDACTION

To indicate the overall heat transfer coefficient (U), the transfer heat of the cold water in shell side and hot water in tubes were considered from (Sepehr et al., 2018) :

$$Q_{cw} = M_{cw} c_{p.cw} (T_{cw.out} - T_{cw.in}) \quad (1)$$

$$Q_{ho} = M_{ho} c_{p.ho} (T_{ho.in} - T_{ho.out}) \quad (2)$$

So the average heat is

$$Q_{ave} = \frac{Q_{wc} + Q_{ho}}{2} \quad (3)$$

The heat balance deviation $\frac{Q_{wc} + Q_{ho}}{\dot{Q}_{ave}}$ necessity be below than 5% and that realized in totally investigational tests. The U can be performed from (Marzouk et al., 2021) :

$$U = \frac{Q_{ave}}{A_s F \Delta T_m} \quad (4)$$

$$A_s = n\pi DL \quad (5)$$

Where A_s is the outer surface where and F is the correlation factor where logarithmic mean temperature difference is

$$\Delta T_{Lm} = \frac{(T_{ho.out} - T_{Cw.out}) - (T_{ho.in} - T_{Cw.in})}{\ln \frac{(T_{ho.out} - T_{Cw.out})}{(T_{ho.in} - T_{Cw.in})}} \quad (6)$$

The effectiveness (ε) reflects the amount of heat that was actually transmitted as a %age of the maximum amount of heat that might be transported $\varepsilon = \frac{\text{actual heat transfer } (\dot{Q})}{\text{maximum haet transfer}(\dot{Q}_{MAX})}$ and the effectiveness (J. Wang et al., 2018) :

$$\varepsilon = \frac{M_{cw} c_{p.cw} (T_{cw.out} - T_{cw.in})}{(Mc_p)_{min} (T_{ho.in} - T_{cw.in})} = \frac{M_{ho} c_{p.ho} (T_{ho.in} - T_{ho.out})}{(Mc_p)_{min} (T_{ho.in} - T_{cw.in})} \quad (7)$$

4. RESULTS AND DISCUSSIONS

4.1 Validation of Numerical Results

For validation of the numerical model, previous experimental study results were compared with the result of this study. A comparison between the overall heat transfer coefficient versus the volume flow rate for experimental and numerical results is introduced in Fig.7 where a comparison between effectiveness versus the volume flow rate for experimental and numerical results is introduced in Fig.8. The average difference between numerical and experiment results for overall heat transfer coefficient and effectiveness around 2.03% and 1.57%, respectively. It is indicated that the differences between the experimental and numerical results were acceptable so that the helical coil heat exchanger model of CFD modeling being considered is efficient and precise.

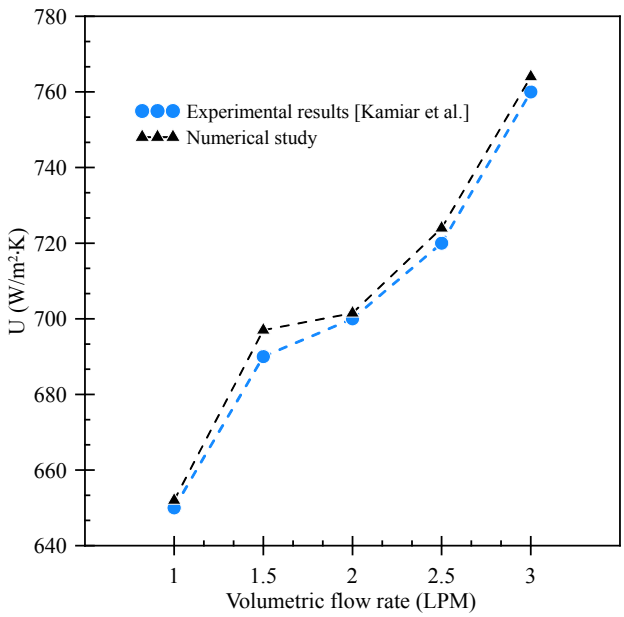

Figure 7. The comparison between the experimental and numerical results for the heat transfer coefficient.

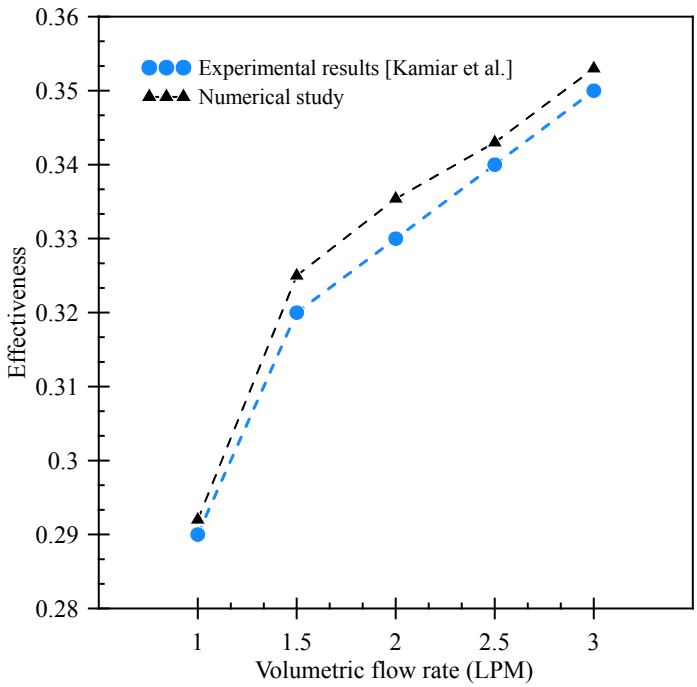

Figure 8. The comparison between the experimental and numerical results for effectiveness.

4.2 Performance Analysis

In this section, the performance parameters such as overall heat transfer coefficient, Nusselt number, effectiveness, and pressure drop of helical coil heat exchanger versus the Reynolds number with a range from 3800 to 18000 were investigated. The relation between the overall heat transfer coefficient and the Reynolds numbers for only helical coil, with twisted tape, and with perforated twisted tape is illustrated in Fig.9. The overall heat transfer coefficient U increase with the rise of Reynolds number where the perforated twisted tape achieved the maximum enhancement of heat transfer coefficient achieving the numbers from 965 to 1250 $W/m^2.K$. The effects of adding twisted tape to the heat exchanger were appeared in the figure where the heat transfer coefficient heat exchanger with twisted tape is higher than the pain helical coil.

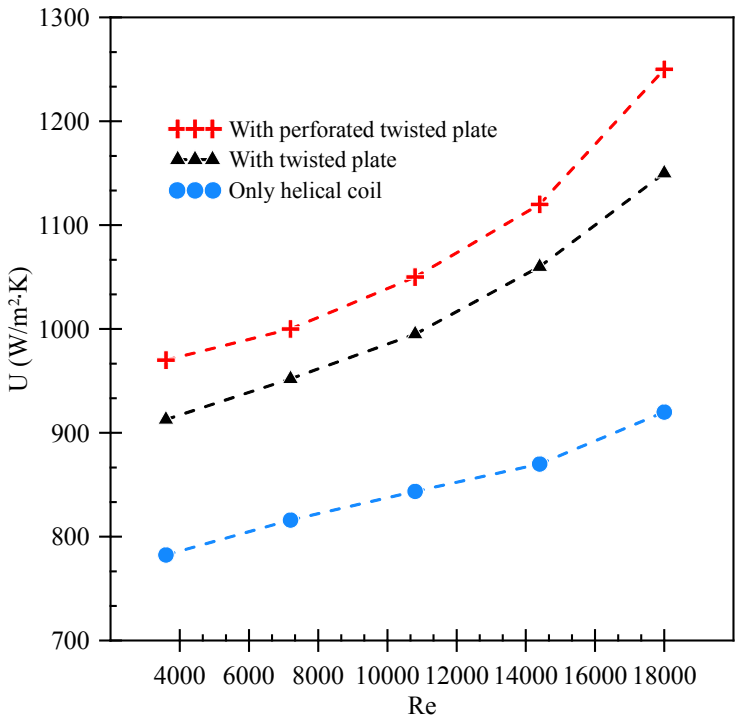

Figure 9. The relation between the overall heat transfer coefficient and the Reynolds numbers for only helical coil, with twisted tape, and with perforated twisted tape.

The variation of the Nussellt number versus the Reynold number is shown in Fig.10 where Nu enhanced with the rise of Reynolds number. It is indicated that the perforated twisted tape has the highest ratio of enhancing Nusselt number following the figures from 65 to 115. This can be explained as the Reynolds number increase the velocity rises so that the turbulence enhanced inside the helical coil so the Nusselt number increases. The holes distributed over the surface of twisted tape increase the velocity and enhance the heat transfer so that the Nusselt number grows.

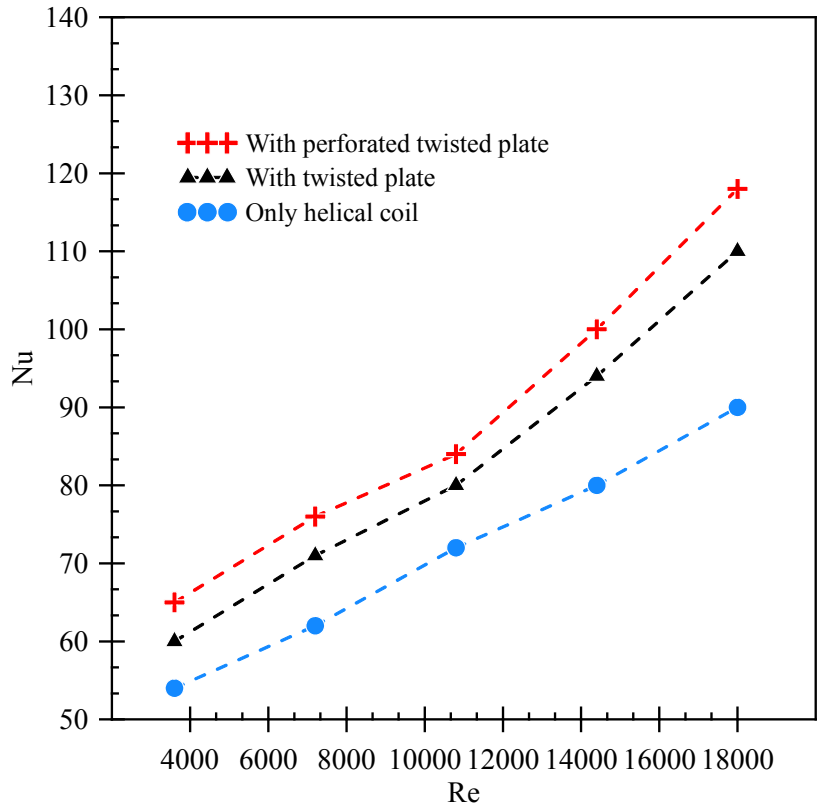

Figure 10. The relation between Nusselt number and the Reynolds numbers for only helical coil, with twisted tape, and with perforated twisted tape.

Fig.11 shows the effectiveness variation versus the Reynolds numbers for only helical coil, with twisted tape, and with perforated twisted tape. Heat exchanger effectiveness increases with the growth of Reynolds number where the perforated twisted tape attained the supreme enhancement of effectiveness reaching the numbers from 0.35 to 0.85.

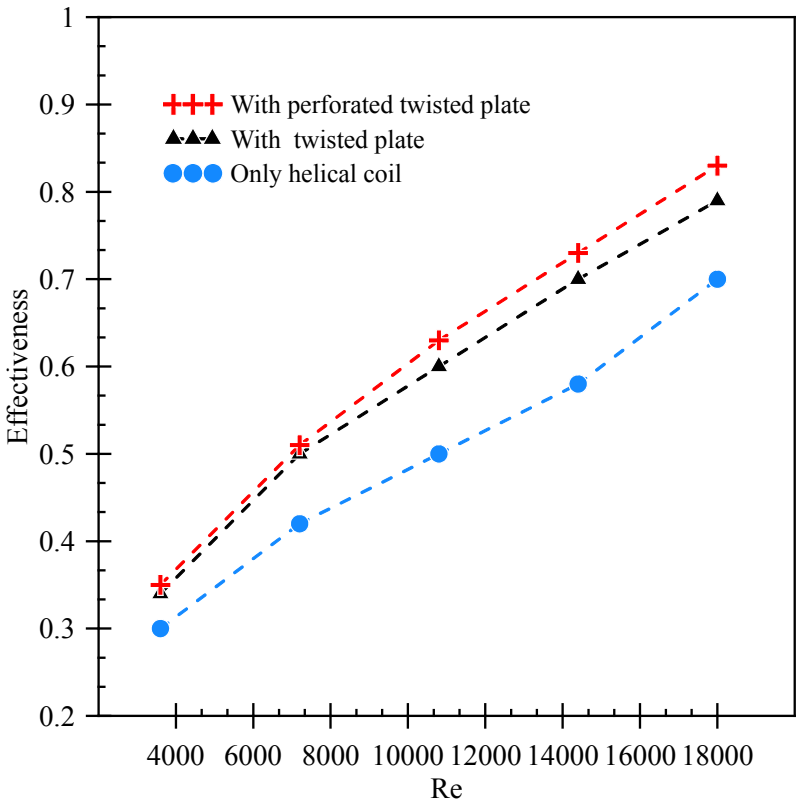

Figure 11. The relation between the effectiveness and the Reynolds numbers for only helical coil, with twisted tape, and with perforated twisted tape.

Fig.12 explains the relation between the pressure drop and the Reynolds numbers for three configurations (eg. only helical coil, with twisted tape, and with perforated twisted tape). It can be indicated that the pressure drop increase with the rise of Reynolds number. The twisted tape configuration has the maximum ratio of pressure drop increase as the complicity of twisted tape rises the pressure drop. It can be observed that the pressure drop in the case of perforated tape is lower than the pressure drop in the case of twisted tape as the holes make the flow inside the helical coil more smoothly.

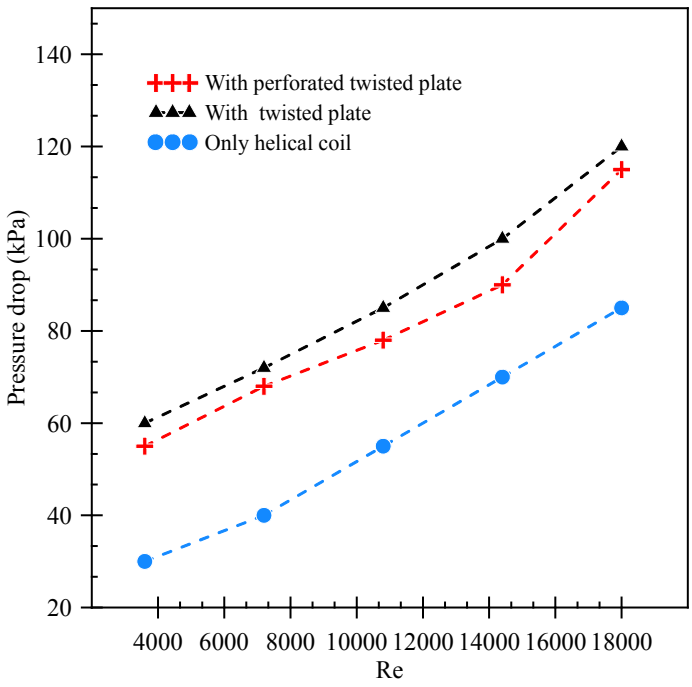

Figure 12. The relation between the pressure drop and the Reynolds numbers for only helical coil, with twisted tape, and with perforated twisted tape.

The temperature distribution of hot water inside the shell side for the three configurations is illustrated in Fig.13 where the effects of inserting perforated twisted tape appear. It is indicated that the temperature distribution in the case of twisted tape is better than the temperature distribution in the case of the only helical coil. The temperature distribution of perforated twisted tape shows more turbulence that leads to more heat transfer enhancement.

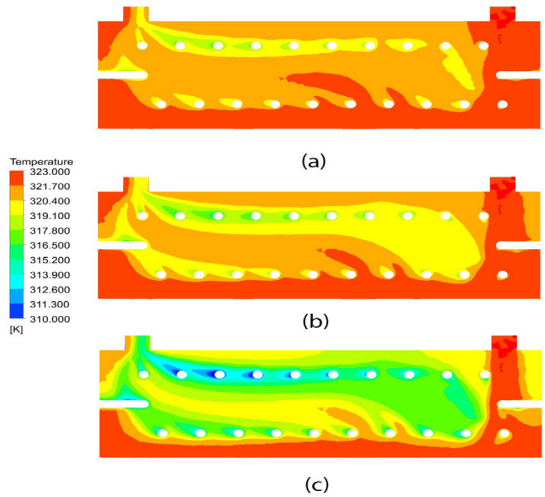

Figure 13. Contours of temperature distribution of hot water for (a) only helical coil, (b) with twisted tape, and (c) with perforated twisted tape.

The temperature distribution of cold water inside the helical coil for the three shapes is demonstrated in Fig.14 where the special influences of injecting perforated twisted tape perform. It is indicated that the temperature distribution in the case of twisted tape is better than the temperature distribution in the case of the only helical coil. The temperature distribution of perforated twisted tape shows more turbulence that leads to more heat transfer enhancement.

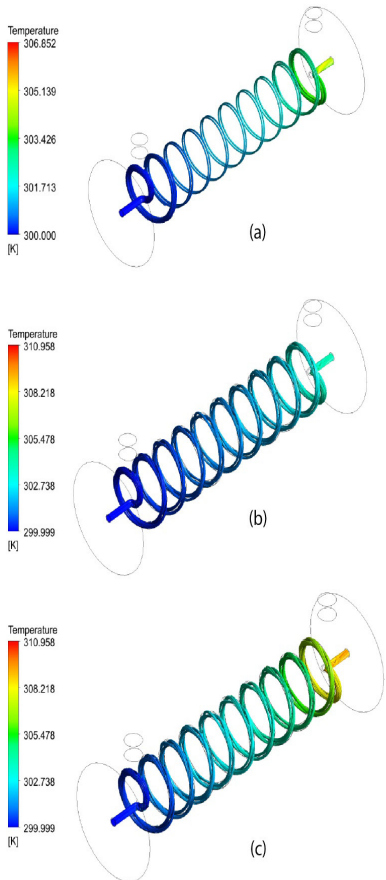

Figure 14. Streamlines of temperature distribution of cold water for (a) only helical coil, (b) with twisted tape, and (c) with perforated twisted tape.

Fig.15 shows the streamlines of velocity distribution where the velocity increases with utilizing the twisted tape. That can be explained as the flow goes through the helical coil the perforated twisted tape force the floe to have twisting passes so that the velocity increase. That leads to enhance the turbulence so that the heat transfer is enhanced from the hot side to the cold side.

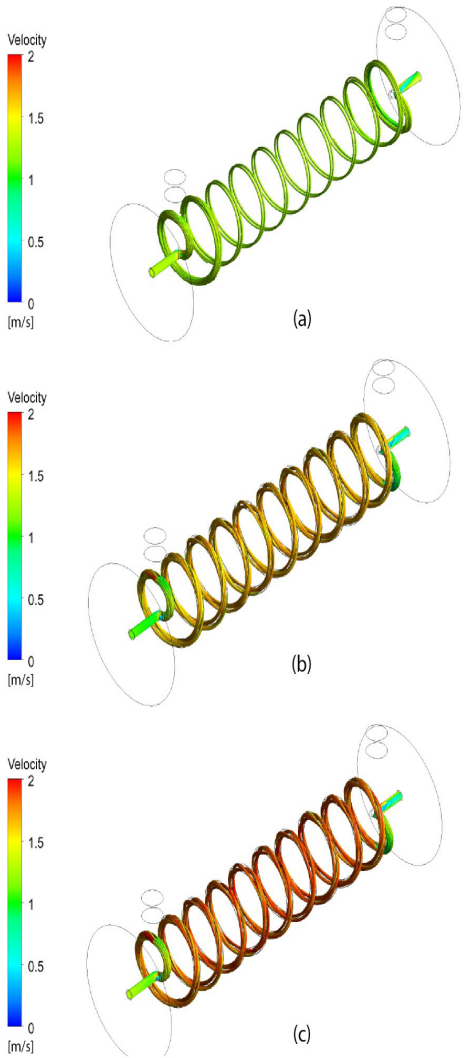

Figure15. Streamlines of the velocity distribution of cold water for (a) only helical coil, (b) with twisted tape, and (c) with perforated twisted tape.

Fig.16 shows the influence of twisted and perforated twisted tape on the pressure distribution inside the helical coil. It is indicated that the twisted tape has the maximum increase in pressure drop. The pressure drop in the case of the perforated tape is less than the pressure drop in the case of twisted tape.

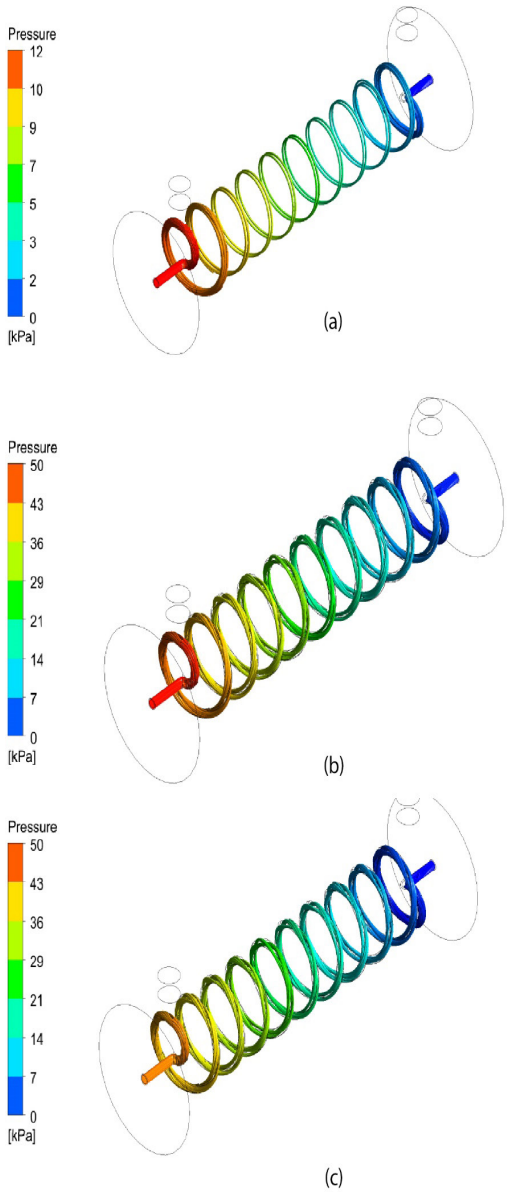

Figure 16. Streamlines of pressure distribution of cold water for (a) only helical coil, (b) with twisted tape, and (c) with perforated twisted tape.

5. CONCLUSION

In this study, the Finite volume method is used to study the effects of twisted tape on heat exchanger performance such as heat transfer coefficient, effectiveness, Nusselt number, and pressure drop. The numerical results were validated with previous experimental results and there was an excessive agreement between the numerical and experimental results. The range of Reynolds numbers is from 3800 to 18000. Contours and streamlines of temperature and pressure were extracted to have a deep understanding of the fluid motion and heat transfer distribution. The results can be concluded in those points:

i. The overall heat transfer coefficient U increase with the rise of Reynolds number where the perforated twisted tape achieved the maximum enhancement of heat transfer coefficient achieving the numbers from 965 to 1250 $W/m^2.K$.

ii. The perforated twisted tape has the highest ratio of enhancing Nusselt number following the numbers from 65 to 115 and this can be explained as the velocity rises, the turbulence level increases.

iii. Heat exchanger effectiveness increases with the growth of Reynolds number where the perforated twisted tape attained the supreme enhancement of effectiveness reaching the numbers from 0.35 to 0.85.

iv. The twisted tape configuration has the maximum ratio of pressure drop increase as the complicity of twisted tape rises the pressure drop.

v. Contours and streamlines of hot and cold water cross the heat exchanger explains the distributions of temperature, velocity, and pressure.

6. REFERENCES

Abu-Hamdeh, N.H., K.H. Almitani, and A. Alimoradi. 2021. Exergetic performance of the helically coiled tube heat exchangers: Comparison the sector-by-sector with tube in tube types. Alexandria Engineering Journal, 60(1), 979-993.

Abu-Hamdeh, N.H., R.A.R Bantan, and I. Tlili. 2020. Analysis of the thermal and hydraulic performance of the sector-by-sector helically coiled tube heat exchangers as a new type of heat exchangers. International Journal of Thermal Sciences, 150, 106229.

Agbossou, A., B. Souyri, and B. Stutz. 2018. Modeling of helical coil heat exchangers for heat pump applications: Analysis of operating modes and distance between heat exchangers. Applied Thermal Engineering, 129, 1068-1078.

Alimoradi, A., and F. Veysi. 2017. Optimal and critical values of geometrical parameters of shell and helically coiled tube heat exchangers. Case Studies in Thermal Engineering, 10, 73-78.

Chagny, C., C. Castelain, and H. Peerhossaimi. 2000. Chaotic heat transfer for heat exchanger design and comparison with a regular regime for a large range of Reynolds numbers. Applied Thermal Engineering, 20(17), 1615-1648.

Eiamsa-Ard, S., and P. Promvonge. 2017. Heat transfer characteristics in a tube fitted with helical screw-tape with/without core-rod inserts. International Communications in Heat and Mass Transfer, 34(2), 176-185.

Farmam, M., M. Khoshvaght-Aliabadi, and M.J. Asadollahzadeh. 2021. Intensified single-phase forces convective heat transfer with helical-twisted tube in coil heat exchangers. Annals of Nuclear Energy, 154, 108108.

Galeazzo, F.C.C., R.Y. Miura, J.A.W. Gut, and C.C. Tadini. 2006. Experimental and numerical heat transfer in a plate heat exchanger. Chemical Engineering Science, 61(21), 7133-7138.

Jean, A., M.K. Nyein, J.Q. Zheng, D.F. Moore, J.D. Joannopoulos, and R. Radovitzky. 2014. An animal-to-human scaling law for blast-induced traumatic brain injury risk assessment. Proceedings of the National Academy of Sciences, 111(43), 15310-15315.

Manglik, R.M., and A.E. Bergles. 2003. Swirl flow heat transfer and pressure drop with twisted-tape inserts. In Advances in Heat Transfer (Vol. 36, pp. 182-266). Elsevier.

Marzouk, S.A., M.M. Abou Al-Sood, M.K. El-Fakharany, and E.M.S. El-Said. 2021. Thermo-hydraulic study in a shell and tube heat exchanger using rod inserts consisting of wire-nails with air injection: Experimental study. International Journal of Thermal Sciences, 161, 106742.

Moawed, M. 2011. Experimental study of forced convection from helical coiled tubes with different parameters. Enerhy Conversion and Management, 52(2), 1150-1156.

Niwalkar, A.F., J.M. Kshirsagar, and K. Kulkarni. 2019. Experimental investigation of heat transfer enhancement in shell and helically coiled tube heat exchaner using SiO2/water nanofluids. Materials Today: Proceedings, 18, 947-962.

Palanisamy, K., and P.C.M. Kumar. 2019. Experimental investigation on convective heat transfer and pressure drop of cone helically coiled tube heat exchanger using carbon nanotubes/water nanofluids. Heliyon. 5(5), e01705.

Panahi, D., and K. Zamzamian. 2017. Heat transfer enhancement of shell-and-coiled tube heat exchanger utilizing helical wire turbulator. Applied Thermal Engineering, 115, 607-615.

Rasheed, A.H., H.B. Alias, and S.D. Salman. 2021. Experimental and numerical investigations of heat transfer enhancement in shell and helically microtube heat exchanger using nanofluids. International Journal of Thermal Sciences, 159, 106547.

Salimpour, M.R. 2009. Heat transfer coefficients of shell and coiled tube heat exchangers. Experimental Thermal and Fluid Science, 33(2), 203-207.

Sepehr, M., S.S. Hashemi, M. Rahjoo, V. Farhangmehr, and A. Alimoradi. 2018. Prediction of heat transfer, pressure drop and entropy generation in shell and helically coiled finned tube heat exchangers. Chemical Engineering Research and Design, 134, 277-291.

Sharifi, K., M. Sabeti, M. Rafiei, A.H. Mohammadi, and L. Shirazi. 2018. Computational fluid dynamics (CFD) technique to study the effects of helical wire inserts on heat transfer and pressure drop in a double pipe heat exchanger. Applied Thermal Engineering, 128, 898-910.

Wang, G., T. Dbouk, D. Wang, Y. Pei, X. Peng, H. Yuan, and S. Xiang. 2020. Experimental and numerical investigation on hydraulic and thermal performance in the tube-side of helically coiled-twisted trilobal tube heat exchanger. International Journal of Thermal Sciences, 153, 106328.

Wang, J., S.S. Hashemi, S. Alahgholi, M. Mehri, M. Safarzadeh, and A. Alimoradi. 2018. Analysis of exergy and energy in shell and helically coiled finned tube heat exchangers and design optimizations. International Journal of Refrigeration, 94, 11-23.